Original article

Dual-phase ^{99m}Tc-MIBI imaging and the expressions of P-gp, GST-π, and MRP1 in hyperparathyroidism

Jianjun Xue[a,*], Yan Liu[a,*], Danrong Yang[b], Yan Yu[b], Qianqian Geng[a], Ting Ji[a], Lulu Yang[a], Qi Wang[a], Yuanbo Wang[a], Xueni Lu[a] and Aimin Yang[a]

Objective The aim of this study was to further elucidate the mechanisms of dual-phase technetium-99m methoxyisobutylisonitrile (^{99m}Tc-MIBI) parathyroid imaging by exploring the association between early uptake results (EUR), delayed uptake results (DUR), and the retention index (RI) in dual-phase ^{99m}Tc-MIBI parathyroid imaging and P glycoprotein (P-gp), multidrug resistance-associated protein 1 (MRP1), and glutathione S-transferase-π (GST-π) expression in hyperparathyroidism (HPT).

Patients and methods Preoperative dual-phase (early and delayed) ^{99m}Tc-MIBI imaging was performed on 74 patients undergoing parathyroidectomy for HPT. EUR, DUR, and RI were calculated. P-gp, MRP1, and GST-π expressions were assessed using immunohistochemistry in resected tissue from HPT and control patients. The association between P-gp, MRP1, and GST-π expressions and EUR, DUR, and RI in HPT was evaluated.

Results The positive rate of dual-phase ^{99m}T c-MIBI imaging was 91.89% (68/74) and the false-negative rate was 8.11% (6/74). P-gp and GST-π expressions were higher in tissues resected from control compared with HPT patients (47.37 and 81.5%, $P < 0.05$); there was no difference in MRP1. EUR were associated with P-gp and GST-π expressions, and DUR were associated with MRP1 expression. There was a significant difference in MRP1 expression between RI greater than or equal to 0 and RI less

than 0. There was no relationship between the sensitivity of dual-phase ^{99m}Tc-MIBI imaging and P-gp, MRP1, and GST-π expressions in resected parathyroid tissue. The six false-negative HPT cases consisted of three P-gp (−)/MRP1 (−) tissues, three P-gp (−)/GST-π (−) tissues, and four MRP1 (−)/GST-π (−) tissues.

Conclusion As P-gp and GST-π expressions were higher in tissues resected from control compared with HPT patients, ^{99m}Tc-MIBI may wash out faster from normal parathyroid tissue surrounding the lesion compared with the lesion itself, facilitating detection. *Nucl Med Commun* 38:868–874 Copyright © 2017 The Author(s). Published by Wolters Kluwer Health, Inc.

[a]Department of Nuclear Medicine, the First Affiliated Hospital of Xi'an Jiaotong University and [b]Department of Public Health, School of Medicine, Xi'an Jiaotong University, Xi'an, Shaanxi, China

Correspondence to Aimin Yang, PhD, MD, Department of Nuclear Medicine, the First Affiliated Hospital of Xi'an Jiaotong University, Xi'an, Shaanxi 710061, China
Tel: + 86 189 912 32193; fax: + 86 298 532 3644;
e-mail: yangaimin@mail.xjtu.edu.cn

*Jianjun Xue and Yan Liu contributed equally to the writing of this article.

Introduction

Hyperparathyroidism (HPT) is a generalized disturbance of calcium and phosphate metabolism that occurs because of the oversecretion of parathyroid hormone (PTH). HPT is characterized by increased serum PTH and calcium levels and decreased serum phosphorus levels. HPT is usually caused by parathyroid adenoma or hyperplastic glands, and rarely by parathyroid carcinomas or parathyroid cysts. In ~85% of cases, primary HPT is attributable to a single benign adenoma [1], and parathyroidectomy is the only effective treatment. In these patients, accurate location of the adenoma is critical for successful surgical intervention. Evidence suggests that B ultrasound,

computed tomography (CT), and MRI have little clinical value in imaging before parathyroidectomy, whereas radionuclide scintigraphy facilitates functional imaging of the parathyroid and is considered the superior imaging modality for preoperative parathyroid localization, especially in ectopic HPT [2,3]. Technetium-99m methoxyisobutylisonitrile (^{99m}Tc-MIBI) was first applied to parathyroid imaging in 1989 [4], and in 1992, dual-phase ^{99m}Tc-MIBI imaging was used to diagnose HPT [5]. Since then, dual-phase ^{99m}Tc-MIBI imaging has shown a high detection rate for parathyroid adenoma, with sensitivity and specificity reported at 39–90% and 94%, respectively [5–10].

^{99m}Tc-MIBI is a lipophilic cation complex; its uptake by a tissue represents the presence of actively functioning mitochondria, and is therefore a measure of a tissue's oxidative burden [11]. The mechanism of dual-phase

^{99m}Tc-MIBI imaging in HPT involves uptake of ^{99m}Tc-MIBI by mitochondria-rich oxyphilic cells in parathyroid adenomas [8,12], whereby ^{99m}Tc-MIBI tracer uptake has been correlated with oxyphilic cell content, volume of parathyroid lesions, and the functional status of parathyroid adenomas [13,14]. Furthermore, ^{99m}Tc-MIBI is more rapidly washed out from healthy thyroid tissue than abnormal parathyroid glands, providing good target-to-background activity [5,15,16]. Although this evidence provides an explanation for the mechanism of dual-phase ^{99m}Tc-MIBI parathyroid imaging, it is likely that other factors are involved. As preoperative localization of abnormal parathyroid glands by dual-phase ^{99m}Tc-MIBI imaging may improve patient outcomes and reduce the duration and cost of surgery for HPT, further investigations are warranted [17,18].

Tissue expression of multidrug-resistant proteins, such as P glycoprotein (P-gp) and multidrug resistance-associated protein 1 (MRP1), may play a role in the mechanism of dual-phase ^{99m}Tc-MIBI parathyroid imaging. Multidrug-resistant proteins are members of the ATP-binding cassette transporter family, which move drugs and their metabolites across cell membranes [7]. In-vivo and in-vitro studies [19–21] show that ^{99m}Tc-MIBI is a suitable transport substrate for P-gp [22,23] and MRP1 [20], and overexpression of P-gp or MRP1 can result in an efflux of ^{99m}Tc-MIBI from tumor cells and lead to false-negative results in dual-phase ^{99m}Tc-MIBI imaging. However, currently, the association between P-gp and MRP1 expression and false-negative results in dual-phase ^{99m}Tc-MIBI imaging is controversial [7,19,24–26].

The glutathione S-transferase (GST) system is involved in the metabolism of various cytotoxic agents and increased drug resistance [26,27]. GST is a multifunctional protein and GST-π is predominantly expressed in tumors. To the authors' knowledge, there are no reports on the association between ^{99m}Tc-MIBI efflux and GST-π expression in the parathyroid.

The aim of this study was to further elucidate the mechanisms of dual-phase ^{99m}Tc-MIBI parathyroid imaging by exploring the association between early uptake results (EUR), delayed uptake results (DUR), and the retention index (RI) in dual-phase ^{99m}Tc-MIBI parathyroid imaging and P-gp, MRP1, and GST-π expressions in HPT.

Patients and methods
Study design
Patients diagnosed with HPT undergoing a parathyroidectomy at our hospital from 2011 to 2015 were eligible for this study. Control tissues were obtained from patients who had their parathyroid glands resected during thyroidectomy for thyroid cancer. Control patients had no history or clinical symptoms of parathyroid disease, and normal serum levels of PTH, calcium, and phosphorus.

Dual-phase ^{99m}Tc-MIBI parathyroid scintigraphy (planar and SPECT/CT) was performed in HPT patients before parathyroidectomy. The presence of P-gp, MRP1, and GST-π proteins was investigated in resected HPT and control parathyroid tissues by immunohistochemistry. The protocol for this study was approved by the Ethics Committee of the Firth Affiliated Hospital, School of Medicine, Xi'an Jiaotong University (Xi'an, China), and written informed consent was obtained from all participants.

Dual-phase ^{99m}Tc-MIBI parathyroid and SPECT/CT imaging
^{9m}TcO$_4^-$ was obtained from a commercial ^{99}Mo/^{99m}Tc generator (Beijing Atom High Tech Co. Ltd, Beijing, China). MIBI was obtained from the Jiangsu Atom Medicine Research Institute, Jiangyuan Pharmaceutical Factory (Wuxi, China). Labeling was performed according to the manufacturer's instructions. Labeling efficiency was more than 95%. Overall, 740–1110 MBq (20–30 mCi) ^{99m}Tc-MIBI was injected intravenously into all HPT patients. After 15 min, dual-phase planar static imaging of the cervical and thoracic area in the anterior view was performed (early phase) using a large-field gamma camera (Siemens, Erlangen, Germany) with a low-energy high-resolution collimator, a 20% energy window centered at a 140-keV photopeak, a 128×128 matrix size, a 1.45 zoom factor, and 500 k counts/view. The delayed phase was performed 120 min after the ^{99m}Tc-MIBI injection. SPECT/CT fusion tomography was performed 30 min after the ^{99m}Tc-MIBI injection using a Symbia T16 scanner (Siemens, Erlangen, Germany).

Immunohistochemistry stain
All resected HPT and control parathyroid tissues were immediately fixed in 10% formalin, embedded in paraffin, and sliced into 4 µm sections. Primary antibodies were the mouse anti-human monoclonal antibodies C494 (anti-P-gp), QCRL1 (anti-MRP1, mouse no. ab3369; Abcam, Shanghai, China), and 353-10 (anti-GST-π, EIivision super kit; Fuzhou Maixin Biotechnology Development Co. Ltd., Fuzhou, China). P-gp, MRP1, and GST-π proteins were detected using the EIivision super kit, according to the manufacturer's instructions. Positive controls were tumor tissue samples known to stain positive for P-gp, MRP1, or GST-π; negative controls were represented by replacing the primary antibody with PBS.

Evaluation of dual-phase ^{99m}Tc-MIBI imaging
Data were evaluated using visual and semiquantitative analysis. For visual evaluation, dual-phase ^{99m}Tc-MIBI images were interpreted independently by two experienced nuclear medicine physicians who were blinded both to the surgical results and to histopathologic diagnoses. A positive dual-phase ^{99m}Tc-MIBI parathyroid image for HPT was

defined as a focal concentration of ^{99m}Tc-MIBI in the early phase, which became increasingly concentrated or showed a fixed concentration in the delayed phase. For semi-quantitative analysis of dual-phase ^{99m}Tc-MIBI positive imaging, a region of interest was defined manually on the lesion in early and delayed imaging; an identical background region of interest was drawn over the deltoid muscle on the contralateral side. The uptake ratio and RI were calculated using the formulae: uptake ratio = mean lesion count/mean contralateral tissue count, RI = (DUR − EUR)/EUR [27,28]. No semiquantitative analysis was carried out for ^{99m}Tc-MIBI negative imaging [29].

Scoring of immunoreactivity

Positive P-gp or MRP1 expression was observed on the cell membrane and/or the cytoplasm (Fig. 1), whereas GST-π was present in the cytoplasm and nucleus (Fig. 2). Immunohistochemical staining was evaluated independently by two investigators using the intensity and the degree of stain. Semiquantification was performed under a transmission electron microscope by randomly selecting 10 high-power fields and counting 100 cells in each field. The intensity of nuclear stain was scored as 0, achromatic; 1, light yellow; 2, brownish yellow; or 3, brown. The degree of nuclear stain was scored as 1 when 0–25% of the nuclei were stained, 2 when 26–75% of the nuclei were stained, and 3 when 76% or more of the nuclei were stained [30]. Both parameters were summed to obtain a final score: less than or equal to 4 was considered a negative result and greater than or equal to 5 was considered a positive result.

Statistical analysis

Data were analyzed using SPSS, version 18.0 (SPSS Inc., Chicago, Illinois, USA). Continuous data are expressed as mean ± SD. Between-sample differences were evaluated using a group-design t-test; differences between multiple samples in the group design were assessed using single-factor analysis of variance (one-way analysis of variance). The χ^2-statistic was used to compare categorical variables. Statistical significance was set at P less than 0.05.

Results

A total of 74 patients diagnosed with HPT undergoing a parathyroidectomy at our hospital were included in this study. Among these patients, there were 28 men and 46 women; patients' mean age was 48.6 ± 15.6 (range: 10–77) years. Preoperative dual-phase ^{99m}Tc-MIBI parathyroid scintigraphy (planar and SPECT/CT) was performed to locate the lesion causing HPT. Postoperative pathology was as follows: parathyroid adenoma: 23 cases, parathyroid hyperplasia: 46 cases, parathyroid carcinoma: four cases, and parathyroid cyst: one case. The control group included 39 samples of normal parathyroid tissue. Among the control patients, there were 13 men and 26 women. The mean age of the patients in the control group was 40.15 ± 12.91 (range: 15–68) years.

^{99m}Tc-MIBI imaging

The positive rate of dual-phase ^{99m}Tc-MIBI imaging was 91.89% (68/74) and the false-negative rate was 8.11% (6/74). Using RI greater than or equal to 0 as the semiquantitative threshold for the presence of HPT in the 68 positive cases in dual-phase ^{99m}Tc-MIBI imaging, the true-positive and false-negative rate was 67.65% (46/68) and 32.35% (22/68), respectively.

P-gp, GST-π, and MRP1 expressions

P-gp, MRP1, and GST-π were detected in parathyroid tissues resected from the control and HPT groups

Fig. 1
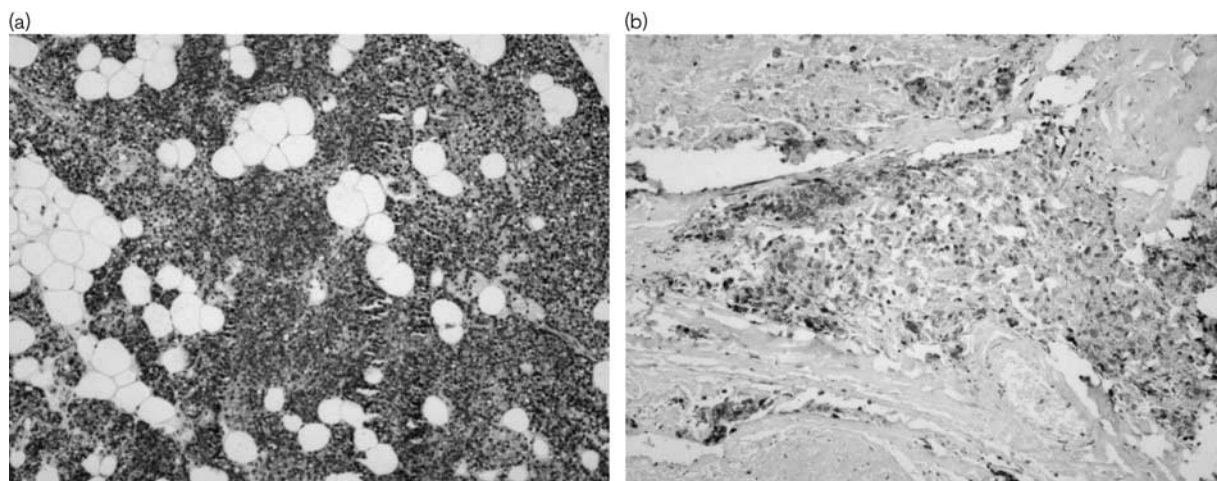
P-gp expression in normal parathyroid (a) and primary hyperparathyroidism (b). P-gp, P-gylcoproetin.

Fig. 2
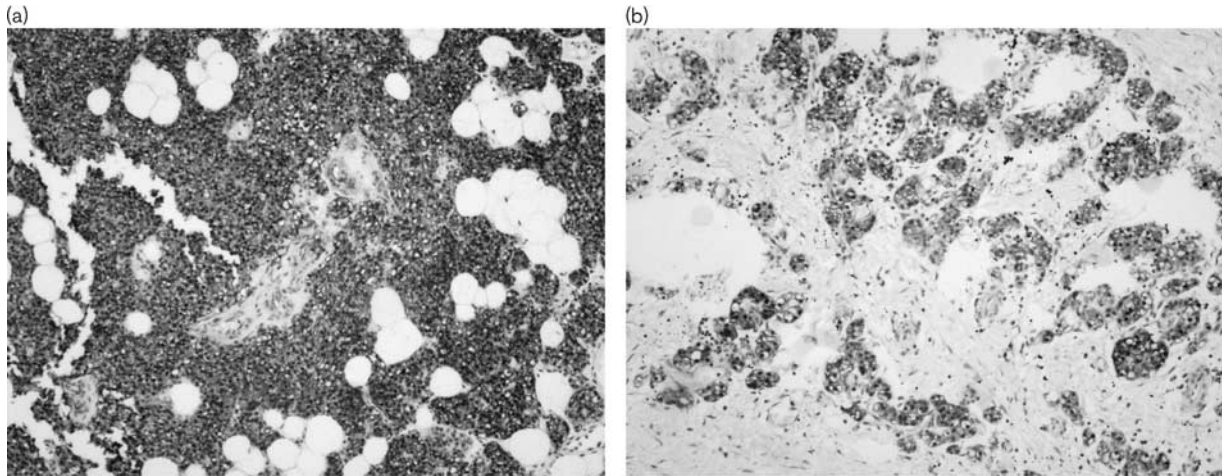
GST-π expression in normal parathyroid (a) and primary hyperparathyroidism (b). GST-π, glutathione S-transferase-π.

Table 1 P-gp, MRP1, and GST-π expressions in hyperparathyroidism and control tissues

Groups	P-gp +	P-gp −	GST-π +	GST-π −	MRP1 +	MRP1 −	Total
Control group	18	20	31	7	10	25	50
HPT group	18	56	28	46	23	51	24
χ^2	5.976		20.474		0.071		
P	0.015		< 0.0001		0.789		

Comparison between the control group and the HPT group: P-gp, $\chi^2 = 5.976$, $P = 0.015$; GST-π, $\chi^2 = 20.474$, $P = 0.000$; MRP1, $\chi^2 = 0.071$, $P = 0.789$.
GST-π, glutathione S-transferase-π; HPT, hyperparathyroidism; MRP1, multidrug resistance-associated protein 1; P-gp, P-gylcoproetin.
Italic values means statistically significant ($P > 0.05$).

(Table 1). The rate of P-gp [control: 47.37% (18/38) vs. HPT: 24.32% (18/74)] and GST-π positive expression [control: 81.58% (31/38) vs. HPT: 37.84% (28/74)] were significantly lower in tissues resected from the HPT group compared with the control group ($\chi^2 = 5.976$, $P = 0.015$ and $\chi^2 = 20.474$, $P < 0.001$). There was no significant difference in the rate of MRP1-positive expression [control: 28.57% (10/35) vs. HPT: 31.08% (23/74)] ($\chi^2 = 0.071$, $P = 0.789$). In the control group, the rate of GST-π-positive expression was significantly higher than the rate of P-gp-positive ($\chi^2 = 10.0$, $P = 0.002$) or MRP1-positive ($\chi^2 = 21.9$, $P < 0.0001$) expression, but there was no significant difference in the rate of P-gp-positive and MRP1-positive expressions ($\chi^2 = 2.75$ $P = 0.097$). There were no significant differences in the rates of P-gp-positive, MRP1-positive, and GST-π-positive expressions in the HPT group ($\chi^2 = 3.173$, $P = 0.205$).

RI in 99mTc-MIBI imaging and P-gp, MRP1, and GST-π expressions in HPT

The correlations between EUR and DUR in dual-phase 99mTC-MIBI imaging and P-gp, MRP1, and GST-π expressions in parathyroid tissue resected from the HPT group are shown in Table 2. EUR were significantly higher in the parathyroid of HPT patients with resected tissues positive for P-gp or GST-π expression than those negative for P-gp or GST-π expression. The relationships between dual-phase 99mTc-MIBI imaging and P-gp/MRP1, P-gp/GST-π, and GST-π/MRP1 expressions in HPT are shown in Tables 3–5, respectively. The six false-negative cases consisted of three P-gp (−)/MRP1 (−) tissues, three P-gp (−)/GST-π (−) tissues, and four MRP1 (−)/GST-π (−) tissues. The relationship between RI in dual-phase 99mTc-MIBI imaging and the expression of P-gp, MRP1, and GST-π in resected tissues is shown in Table 6. There was a significant difference in MRP1 expression between the RI greater than or equal to 0 and the RI less than 0 groups.

Discussion

The aim of this study was to further elucidate the mechanisms of dual-phase 99mTc-MIBI parathyroid imaging by exploring the association between EUR, DUR, and RI and P-gp, MRP1, and GST-π expressions in HPT. Findings showed that the positive rate of dual-phase 99mTc-MIBI imaging for detecting parathyroid lesions in our patient population was 91.89% (68/74) and the false-negative rate was 8.11% (6/74). P-gp, MRP1, and GST-π expressions were low in tissues resected from patients with HPT. EUR in dual-phase 99mTc-MIBI imaging were associated with P-gp and GST-π expressions, and DUR were associated with MRP1 expression. There was no relationship between the sensitivity of dual-phase 99mTc-MIBI imaging and P-gp, MRP1, and GST-π expressions in resected parathyroid tissue.

These findings may further explain the mechanism of localization of parathyroid lesions by dual-phase 99mTc-MIBI imaging. Our results showed that the

Table 2   Relationship between early uptake results, delayed uptake results, and retention index and P-gp, MRP1, and GST-π expressions in hyperparathyroidism

$^{99m}T_C$-MIBI	P-gp		GST-π		MRP1	
	+ (n = 18)	− (n = 56)	+ (n = 28)	− (n = 46)	+ (n = 23)	− (n = 51)
EUR	2.678 ± 1.510*	1.848 ± 0.866*	2.408 ± 1.276^	1.832 ± 0.938^	1.843 ± 1.314	2.144 ± 1.000
DUR	3.310 ± 2.549	2.431 ± 1.489	3.161 ± 2.102	2.330 ± 1.574	1.986 ± 1.933#	2.942 ± 1.710#
RI	0.142 ± 0.448	0.271 ± 0.734	0.297 ± 0.616	0.205 ± 0.712	−0.416 ± 0.836†	0.367 ± 0.551†

DUR, delayed uptake results; EUR, early uptake results; GST-π, glutathione S-transferase-π; MRP1, multidrug resistance-associated protein 1; P-gp, P-gylcoproetin; RI, retention index; ^{99m}Tc-MIBI, technetium-99m methoxyisobutylisonitrile.
*$t = -2.093$, $P = 0.005$.
^$t = -2.229$, $P = 0.029$.
#$t = 2.135$, $P = 0.036$.
†$t = -2.497$, $P = 0.015$.

Table 3   Relationship between dual-phase ^{99m}Tc-MIBI imaging and P-gp and MRP1 expressions in hyperparathyroidism

Results of dual-phase ^{99m}Tc-MIBI imaging	Total	Group 1 P-gp (+)/MRP1 (+)	Group 2 P-gp (+)/MRP1 (−)	Group 3 P-gp (−)/MRP1 (+)	Group 4 P-gp (−)/MRP1 (−)
Positive	68	4	12	17	35
Negative	6	1	1	1	3

MRP1, multidrug resistance-associated protein 1; P-gp, P-gylcoproetin; ^{99m}Tc-MIBI, technetium-99m methoxyisobutylisonitrile.

Table 4   Relationship between dual-phase ^{99m}Tc-MIBI imaging and P-gp and GST-π expressions in hyperparathyroidism

Results of dual-phase ^{99m}Tc-MIBI imaging	Total	Group 1 P-gp (+)/GST-π (+)	Group 2 P-gp (+)/GST-π (−)	Group 3 P-gp (−)/GST-π (+)	Group 4 P-gp (−)/GST-π (−)
Positive	68	7	9	20	32
Negative	6	0	2	1	3

GST-π, glutathione S-transferase-π; P-gp, P-gylcoproetin; ^{99m}Tc-MIBI, technetium-99m methoxyisobutylisonitrile.

Table 5   Relationship between dual-phase ^{99m}Tc-MIBI imaging and GST-π and MRP1 expressions in hyperparathyroidism

Results of dual-phase ^{99m}Tc-MIBI imaging	Total	Group 1 GST-π (+)/MRP1 (+)	Group 2 GST-π (+)/MRP1 (−)	Group 3 GST-π (−)/MRP1 (+)	Group 4 GST-π (−)/MRP1 (−)
Positive	68	9	18	12	29
Negative	6	1	0	1	4

GST-t, glutathione S-transferase-π; MRP1, multidrug resistance-associated protein 1; ^{99m}Tc-MIBI, technetium-99m methoxyisobutylisonitrile.

Table 6   Relationship between retention index and P-gp, MRP1, and GST-π expressions in hyperparathyroidism

Groups	N	P-gp		MRP1		GST-π	
		+	−	+	−	+	−
RI ≥ 0	46	11	35	9	37	18	28
RI < 0	22	5	17	12	10	9	13
χ^2			0.012		8.276		0.02
P			0.914		0.004		0.889

GST-π, glutathione S-transferase-π; MRP1, multidrug resistance-associated protein 1; P-gp, P-gylcoproetin.

expressions of P-gp, MRP1, and GST-π were lower in tissues resected from patients with HPT than in control tissues. This suggests that ^{99m}Tc-MIBI may wash out faster from the normal parathyroid tissue surrounding the lesion compared with the lesion itself, facilitating detection.

The current study showed no relationship between the sensitivity of dual-phase ^{99m}Tc-MIBI imaging and P-gp, MRP1, and GST-π expressions in resected parathyroid tissue. There are many factors that influence the diagnosis and location of parathyroid lesions in HPT by dual-phase ^{99m}Tc-MIBI imaging, including the size of the parathyroid gland, blood flow in the parathyroid adenoma, and the secretory function and the activity of the parathyroid cells [14,31–35]. In addition, autoimmune thyroid disease [16] and nonsteroidal anti-inflammatory drugs [36] may reduce the sensitivity of Tc-99m MIBI parathyroid scintigraphy. Kao et al. [37] reported that eight parathyroid adenomas with significant P-gp or MRP expression were not detected by ^{99m}Tc-MIBI imaging, but focal ^{99m}Tc-MIBI uptake could be found in 39 parathyroid adenomas negative for both P-gp and MRP expressions. The authors concluded that the sensitivity of ^{99m}Tc-MIBI parathyroid imaging for localizing

Fig. 3
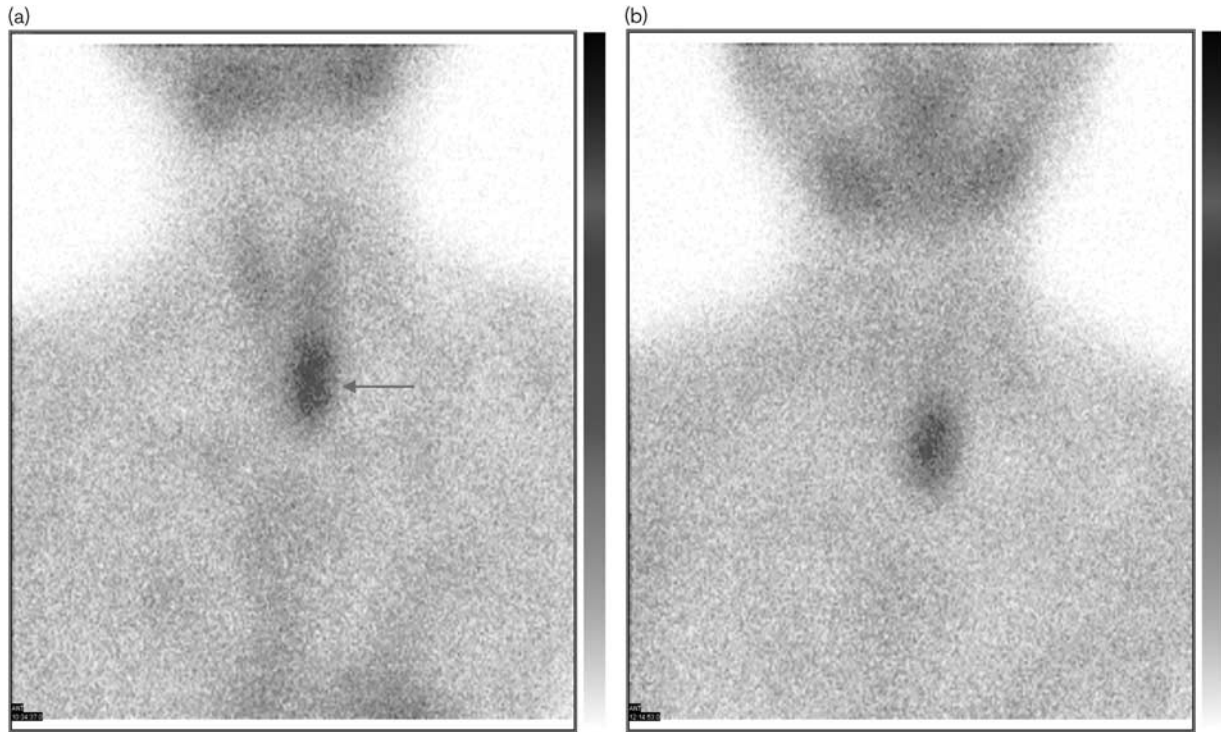
P-gp (+)/MRP1 (+)/GST-π (+), ^{99m}Tc-MIBI imaging 15 min (a) and 2 h (b). EUR = 2.07, DUR = 2.03. DUR, delayed uptake results; EUR, early uptake results; GST-π, glutathione S-transferase-π; MRP1, multidrug resistance-associated protein 1; P-gp, P-gylcoproetin; ^{99m}Tc-MIBI, technetium-99m methoxyisobutylisonitrile. Arrow shows parathyroid tumor.

parathyroid adenomas was limited by the presence of P-gp or MRP. Although several studies reported similar results [34,38], in accordance with our findings, others showed that P-gp or MRP1 expression was not related to the uptake of ^{99m}Tc-MIBI in parathyroid tumors [19,26, 39] (Fig. 3).

The results of this study indicate that EUR in dual-phase ^{99m}Tc-MIBI imaging were associated with P-gp and GST-π expression, and DUR were associated with MRP1 expression. The data suggest that P-gp, MRP1, and GST-π play temporally distinct roles in ^{99m}Tc-MIBI efflux. In the early phase, the washout of ^{99m}Tc-MIBI is influenced by P-gp and GST-π, whereas washout in the delayed phase is influenced by MRP1. Furthermore, there were no significant differences in P-gp or GST-π expression and RI in dual-phase ^{99m}Tc-MIBI imaging. This may be because low positive expression of P-gp and GST-π in parathyroid lesions of HPT patients has little influence on ^{99m}Tc-MIBI efflux. However, these data should be interpreted with caution as the determination of the lesion boundary when identifying the region of interest was subjective, which may introduce some inaccuracy when calculating the RI.

Conclusion

P-gp, MRP1, and GST-π expressions were low in tissues resected from patients with HPT compared with control tissues. This may further explain the mechanism of localization of parathyroid lesions by dual-phase ^{99m}Tc-MIBI imaging. ^{99m}Tc-MIBI may wash out faster from the normal parathyroid tissue surrounding the lesion compared with the lesion itself, facilitating detection. However, our findings suggest that there is no relationship between the sensitivity of dual-phase ^{99m}Tc-MIBI imaging and P-gp, MRP1, and GST-π expressions in resected parathyroid tissue from patients with HPT.

References
1 Fraker DL, Harsono H, Lewis R. Minimally invasive parathyroidectomy: benefits and requirements of localization, diagnosis, and intraoperative PTH monitoring. long-term results. *World J Surg* 2009; **33**:2256–2265.
2 Phillips CD, Shatzkes DR. Imaging of the parathyroid glands. *Semin Ultrasound CT MR* 2012; **33**:123–129.
3 Hindié E, Zanotti-Fregonara P, Tabarin A, Rubello D, Morelec I, Wagner T, *et al*. The role of radionuclide imaging in the surgical management of primary hyperparathyroidism. *J Nucl Med* 2015; **56**:737–744.

4   Coakley AJ, Kettle AG, Wells CP, O'Doherty MJ, Collins RE. 99Tcm sestamibi – a new agent for parathyroid imaging. *Nucl Med Commun* 1989; **10**:791–794.

5   Taillefer R, Boucher Y, Potvin C, Lambert, R. Detection and localization of parathyroid adenomas in patients with hyperparathyroidism using a single radionuclide imaging procedure with technetium-99m-sestamibi (double-phase study). *J Nucl Med* 1992; **33**:1801–1807.

6   Rao VV, Chiu ML, Kronauge JF, Piwnica-Worms D. Expression of recombinant human multidrug resistance P-glycoprotein in insect cells confers decreased accumulation of technetium-99m-sestamibi. *J Nucl Med* 1994; **35**:510–515.

7   Sun SS, Shiau YC, Lin CC, Kao A, Lee CC. Correlation between P-glycoprotein (P-gp) expression in parathyroid and Tc-99m MIBI parathyroid image findings. *Nucl Med Biol* 2001; **28**:929–933.

8   Piñero A, Rodriguez JM, Martinez-Barba E, Canteras M, Stiges-Serra A, Parrilla P. Tc99m-sestamibi scintigraphy and cell proliferation in primary hyperparathyroidism: a causal or casual relationship? *Surgery* 2003; **134**:41–44.

9   Gotthardt M, Lohmann B, Behr TM, Bauhofer A, Franzius C, Schipper ML, *et al*. Clinical value of parathyroid scintigraphy with technetium-99m methoxyisobutylisonitrile: discrepancies in clinical data and a systematic metaanalysis of the literature. *World J Surg* 2004; **28**:100–107.

10   Treglia G, Sadeghi R, Schalin-Jäntti C, Caldarella C, Ceriani L, Giovanella L, *et al*. Detection rate of ^{99m}Tc-MIBI single photon emission computed tomography (SPECT)/CT in preoperative planning for patients with primary hyperparathyroidism: a meta-analysis. *Head Neck* 2015; **38**:E2159–E2172.

11   Giovanella L, Campenni A, Treglia G, Verburg FA, Trimboli P, Ceriani L, *et al*. Molecular imaging with ^{99m}Tc-MIBI and molecular testing for mutations in differentiating benign from malignant follicular neoplasm: a prospective comparison. *Eur J Nucl Med Mol Imaging* 2016; **43**:1–9.

12   Bénard F, Lefebvre B, Beuvon F, Langlois MF, Bisson G. Rapid washout of technetium-99m-MIBI from a large parathyroid adenoma. *J Nucl Med* 1995; **36**:241–243.

13   Pons F, Torregrosa JV, Vidal-Sicart S, Sabater L, Fuster D, Fernández-Cruz L, *et al*. Preoperative parathyroid gland localization with technetium-99m sestamibi in secondary hyperparathyroidism. *Eur J Nucl Med* 1997; **24**:1494–1498.

14   Melloul M, Paz A, Koren R, Cytron S, Feinmesser R, Gal R. ^{99m}Tc-MIBI scintigraphy of parathyroid adenomas and its relation to tumour size and oxyphil cell abundance. *Eur J Nucl Med* 2001; **28**:209–213.

15   O'Doherty MJ, Kettle AG, Wells P, Collins RE, Coakley AJ. Parathyroid imaging with technetium-99m-sestamibi: preoperative localization and tissue uptake studies. *J Nucl Med* 1992; **33**:313–318.

16   Hwang SH, Rhee Y, Yun M, Yoon JH, Lee JW, Cho A. Usefulness of SPECT/CT in parathyroid lesion detection in patients with thyroid parenchymal ^{99m}Tc-sestamibi retention. *Nucl Med Mol Imaging* 2017; **51**:1–8.

17   Lenz JI, Jacobs JM, Op de Beeck B, Huyghe IA, Pelckmans PA, Moreels TG. Acute necrotizing pancreatitis as first manifestation of primary hyperparathyroidism. *World J Gastroenterol* 2010; **16**:2959–2962.

18   Bae EH, Kim HS, Kim MJ, Kang YU, Kim YH, Kim CS, *et al*. Hypercalcemia in a patient with polycythemia vera. *Chonnam Med J* 2012; **48**:128–129.

19   Jorna FH, Hollema H, Hendrikse HN, Bart J, Brouwers AH, Plukker JT. P-gp and MRP1 expression in parathyroid tumors related to histology, weight and ^{99m}Tc-sestamibi imaging results. *Exp Clin Endocrinol Diabetes* 2009; **117**:406–412.

20   Hendrikse NH, Franssen EJ, van der Graaf WT, Vaalburg W, de Vries EG. Visualization of multidrug resistance in vivo. *Eur J Nucl Med* 1999; **26**:283–293.

21   Hendrikse NH. Monitoring interactions at ATP-dependent drug efflux pumps. *Curr Pharm Des* 2000; **6**:1653–1668.

22   Arbab AS, Koizumi K, Toyama K, Araki T. Uptake of technetium-99m-tetrofosmin, technetium-99m-MIBI and thallium-201 in tumor cell lines. *J Nucl Med* 1996; **37**:1551–1556.

23   Ballinger JR, Bannerman J, Boxen I, Firby P, Hartman NG, Moore MJ. Technetium-99m-tetrofosmin as a substrate for P-glycoprotein: in vitro studies in multidrug-resistant breast tumor cells. *J Nucl Med* 1996; **37**:1578–1582.

24   Gupta Y, Ahmed R, Happerfield L, Pinder SE, Balan KK, Wishart GC. P-glycoprotein expression is associated with sestamibi washout in primary hyperparathyroidism. *Br J Surg* 2007; **94**:1491–1495.

25   Ugur O, Bozkurt MF, Hamaloglu E, Sokmensuer C, Etikan I, Ugur Y, *et al*. Clinicpathologic and radiopharmacokinetic factors affecting gamma probe-guided parathyroidectomy. *Arch Surg* 2004; **139**:1175–1179.

26   Turgut B, Elagoz S, Erselcan T, Koyuncu A, Dokmetas HS, Hasbek Z, *et al*. Preoperative localization of parathyroid adenomas with technetium-99m methoxyisobutylisonitrile imaging: relationship with P-glycoprotein expression, oxyphilic cell content, and tumoral tissue volume. *Cancer Biother Radiopharm* 2006; **21**:579–590.

27   Xue JJ, Yang AM, Zhang FR, Wang HY, Deng Y, Li JH, *et al*. Correlation between uptake of 99Tcm-MIBI and expression of multidrug resistant protein in primary lung cancer. *Chin J Med Imaging Technol* 2006; **22**:1090–1094.

28   Yang A, Xue J, Li X, Yu Y, Deng H, Hu G, *et al*. Experimental and clinical observations of ^{99m}Tc-MIBI uptake correlate with P-glycoprotein expression in lung cancer. *Nucl Med Commun* 2007; **28**:696–703.

29   Kurata S, Ushijima K, Kawahara A, Kaida H, Kawano K, Hirose Y, *et al*. Assessment of ^{99m}Tc-MIBI SPECT(/CT) to monitor multidrug resistance-related proteins and apoptosis-related proteins in patients with ovarian cancer: a preliminary study. *Ann Nucl Med* 2015; **29**:643–649.

30   Wu HS, Liu YC, Kao A, Wang JJ, Ho ST. Using technetium 99m-tetrofosmin parathyroid imaging to detect parathyroid adenoma and its relation to P-glycoprotein expression. *Surgery* 2002; **132**:456–460.

31   Carcangiu ML, Chambers JT, Voynick IM, Pirro M, Schwartz PE. Immunohistochemical evaluation of estrogen and progesterone receptor content in 183 patients with endometrial carcinoma. Part I: clinical and histologic correlations. *Am J Clin Pathol* 1990; **94**:247–254.

32   Leslie WD, Riese KT, Dupont JO, Peterdy AE. Parathyroid adenomas without sestamibi retention. *Clin Nucl Med* 1995; **20**:699–702.

33   Rauth JD, Sessions RB, Shupe SC, Ziessman HA. Comparison of Tc-99m MIBI and Tl-201/Tc-99m pertechnetate for diagnosis of primary hyperparathyroidism. *Clin Nucl Med* 1996; **21**:602–608.

34   Pons F, Torregrosa JV, Fuster D. Biological factors influencing parathyroid localization. *Nucl Med Commun* 2003; **24**:121–124.

35   Arbab AS, Ueki J, Koizumi K, Araki T. Effects of extracellular Na + and Ca^{2+} ions and Ca^{2+} channel modulators on the cell-associated activity of ^{99m}Tc-MIBI and ^{99m}Tc-tetrofosmin in tumour cells. *Nucl Med Commun* 2003; **24**:155–166.

36   Araz M, Çayir D, Erdoğan M, Uçan B, Çakal E. Factors affecting the sensitivity of Tc-99m methoxyisobutylisonitrile dual-phase parathyroid single photon emission computed tomography in primary hyperparathyroidism. *Nucl Med Commun* 2017; **38**:117–123.

37   Kao A, Shiau YC, Tsai SC, Wang JJ, Ho ST. Technetium-99m methoxyisobutylisonitrile imaging for parathyroid adenoma: relationship to P-glycoprotein or multidrug resistance-related protein expression. *Eur J Nucl Med* 2002; **29**:1012–1015.

38   Yamaguchi S, Yachiku, S, Hashimoto H, Kaneko S, Nishihara M, Niibori D, *et al*. Relation between technetium 99m-methoxyisobutylisonitrile accumulation and multidrug resistance protein in the parathyroid glands. *World J Surg* 2002; **26**:29–34.

39   Bhatnagar A, Vezza PR, Bryan JA, Atkins FB, Ziessman HA. Technetium-99m-sestamibi parathyroid scintigraphy: effect of P-glycoprotein, histology and tumor size on detectability. *J Nucl Med* 1998; **39**:1617–1620.